Random non-proportional fatigue tests with planar tri-axial fatigue testing machine

T. Inoue, R. Nagao, N. Takeda

Hitachi, Ltd., Research & Development Group, Center for Technology Innovation – Mechanical Engineering, 832-2 Horiguchi, Ibaraki, 312-0034 Japan

takeshi.inoue.sb@hitachi.com, riichi.nagao.ac@hitachi.com, norio.takeda.uf@hitachi.com

ABSTRACT. Complex stresses, which occur on the mechanical surfaces of transport machinery in service, bring a drastic degradation in fatigue life. However, it is hard to reproduce such complex stress states for evaluating the fatigue life with conventional multiaxial fatigue machines. We have developed a fatigue testing machine that enables reproduction of such complex stresses. The testing machine can reproduce arbitrary in-plane stress states by applying three independent loads to the test specimen using actuators which apply loads in the 0, 45, and 90 degree directions. The reproduction was tested with complex stress data obtained from the actual operation of transport machinery. As a result, it was found that the reproduced stress corresponded to the measured stress with an error range of less than 10 %. Then, we made a comparison between measured fatigue lives under random non-proportional loading conditions and predicted fatigue lives. It was found that predicted fatigue lives with σ_{cr}, stress on critical plane, were over a factor of 10 against measured fatigue lives. On the other hand, predicted fatigue lives with σ_{ma}, stress in consideration of a non-proportional level evaluated by using amplitude and direction of principal stress, were within a factor of 3 against measured fatigue lives.

KEYWORDS. Fatigue; Non-proportional; Random; Plane stress; Fatigue life prediction; Testing machine.

Citation: Inoue, T., Nagao, R., Takeda, N., Random non-proportional fatigue tests with planar tri-axial fatigue testing machine, Frattura ed Integrità Strutturale, 38 (2016) 259-265.

Received: 26.07.2016
Accepted: 28.08.2016
Published: 01.10.2016

INTRODUCTION

The main objective of this study is to develop a fatigue testing machine that enables reproduction of complex stresses occurring on the mechanical surfaces of transport machinery in service such as automobiles and railway vehicles.

It is well-known that non-proportional loading generating such complex stresses brings a drastic degradation in fatigue life [1, 2]. Methods for prediction of fatigue life in consideration of life degradation have been proposed using fatigue testing results with two types of fatigue testing machines, a planar cross axial testing machine and an axial and torsion testing

machine [3, 4].
However, it is hard to reproduce such complex stress states with conventional multiaxial fatigue testing machines.
In this study, we have developed a fatigue testing machine that enables generation of arbitrary in-plane stress states which occur on a mechanical surface where fatigue crack initiates. Also, fatigue tests under random non-proportional loading conditions were performed with the advanced tasting machine.

EXPERIMENTAL METHOD

Testing Machine

The advanced testing machine has three structural features.
First, the advanced testing machine consists of mechanical structures for generating three independent loads in the 0, 45, and 90 degree directions using actuators which apply loads. For generating arbitrary in-plane stress states, namely, σ_x, σ_y and τ_{xy} in the xy plane, on the test specimen, three independent loads in the same plane are required. Stress states generated by conventional multiaxial fatigue testing machines are shown in Fig. 1. σ_1, σ_2, and θ_1 in Fig. 1 are the maximum principal stress, the minimum principal stress, and the maximum principal stress direction in the xy plane, respectively. Since conventional machines consist of mechanical structures for applying two independent loads to the test specimen, stress states to be generated are limited. θ_1 generated by the planar cross axial testing machine is limited to 0 or 90 degrees as shown in Fig. 1 (a). When the axial stress direction is x, σ_y generated by the axial and torsion testing machine is limited to 0 as shown in Fig. 1 (b). On the other hand, in the advanced testing machine, the structure for applying the load in the 45 degree direction is added to the planar cross axial fatigue testing machine. σ_1, σ_2, and θ_1 generated by the advanced testing machine are therefore described in the following expression:

$$\sigma_{1(2)} = \frac{\sigma_0 + \sigma_{90} + \sigma_{45}}{2} \pm \frac{\sqrt{(\sigma_0 - \sigma_{90})^2 + \sigma_{45}^2}}{2} \tag{1}$$

$$\theta_1 = \frac{1}{2}\tan^{-1}\left(\frac{\sigma_{45}}{\sigma_0 - \sigma_{90}}\right) \tag{2}$$

where σ_0, σ_{90}, and σ_{45} are stresses generated by loads in the 0, 90, and 45 degree directions, respectively. The limit of θ_1 is eliminated for the advanced testing machine. In other words, this testing machine could generate arbitrary in-plane stress states.

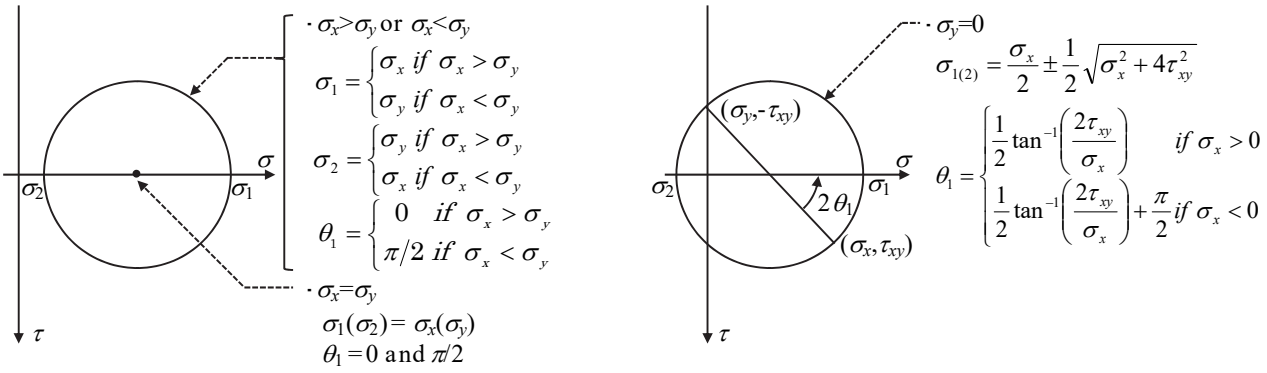

(a) Planar cross axial testing machine. (b) Axial and torsion testing machine.

Figure 1: Stress states under Mohr's stress circle generated with each testing machine.

Second, the advanced testing machine generates loads with mechanical structures each of which includes an actuator on one side and a reaction wall on the other side. These structures enable simplification of actuator control.
Third, the advanced testing machine consists of a fixed frame which forms a 45 degree test axis and two movable frames which form 0 and 90 degree test axes. These structures enable prevention of a misalignment between the center of the specimen being shifted by loading to one direction and each loading axis. As a result, the prevention of misalignment can avoid a bending stress and a fracture of the test specimen by that bending stress.
Fig. 2 and Tab. 1 show the advanced testing machine structures and specifications. Two frames, each of which has an actuator and a reaction wall, are installed on the fixed frame trough linear motion guides. An electro-hydraulic control system is installed in the testing machine. This testing machine was manufactured by Shimadzu Corporation.

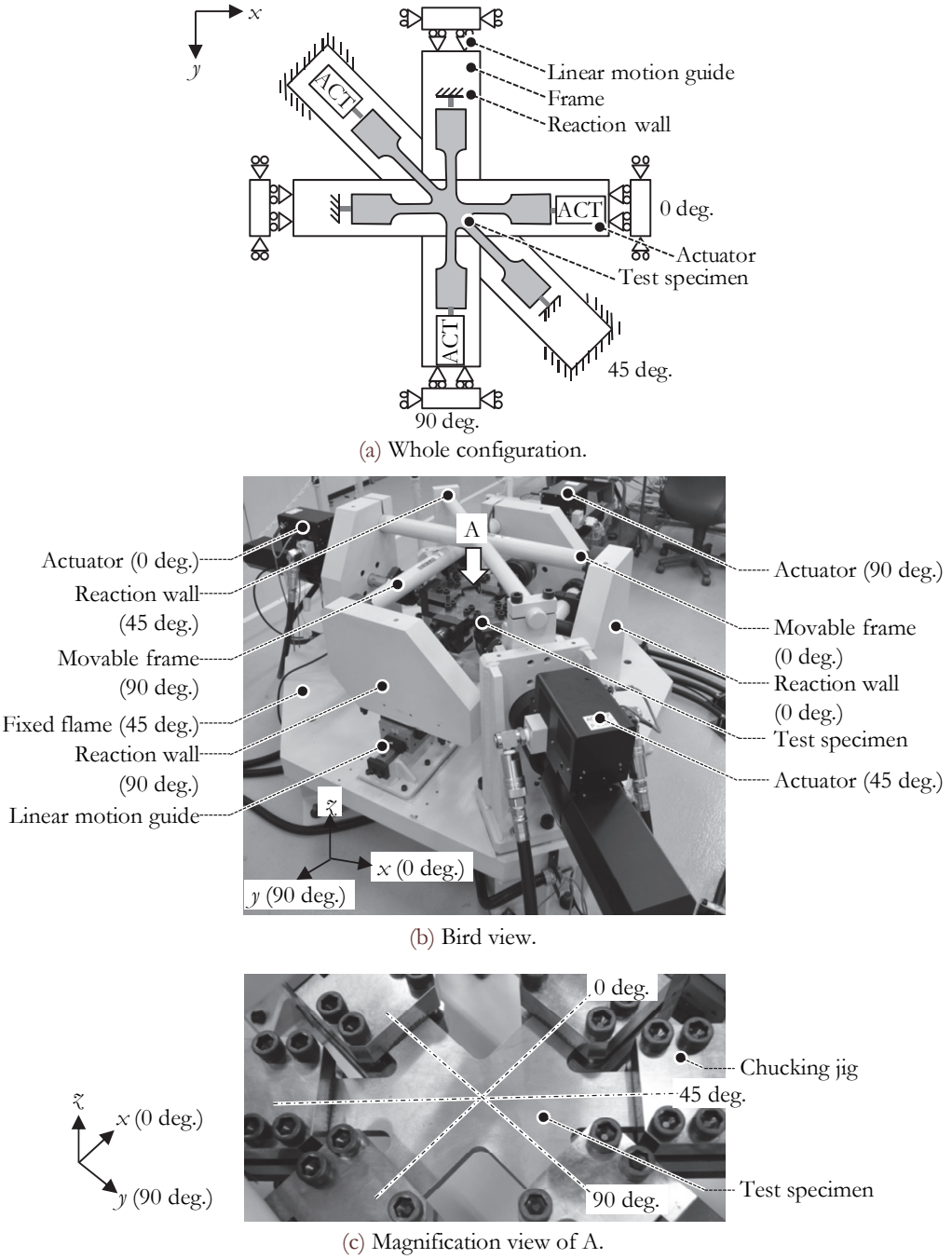

Figure 2: Planar tri-axial fatigue testing machine.

Max. load	±50 kN
Max. stroke	±50 mm
Max. frequency under uniaxial loading	10 Hz
Max. frequency under tri-axial loadings	5 Hz

Table 1: Specifications of planar tri-axial fatigue testing machine.

Test Specimen

Two types of specimens made of SS400 were used as shown in Fig. 3. One was designed as a cylindrical projection on the center of the specimen as shown in Fig. 3 (b). The other was flat shaped as shown in Fig. 3 (c). The chemical composition and mechanical properties of SS400 are shown in Tabs. 2 and 3.

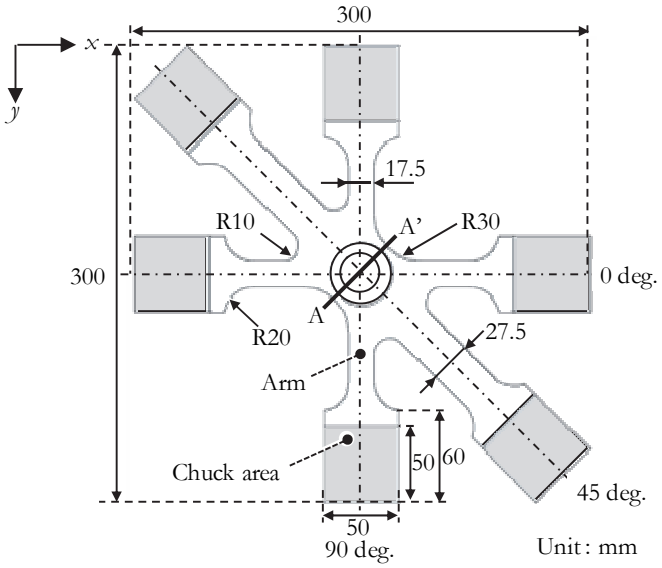

(a) Top view.

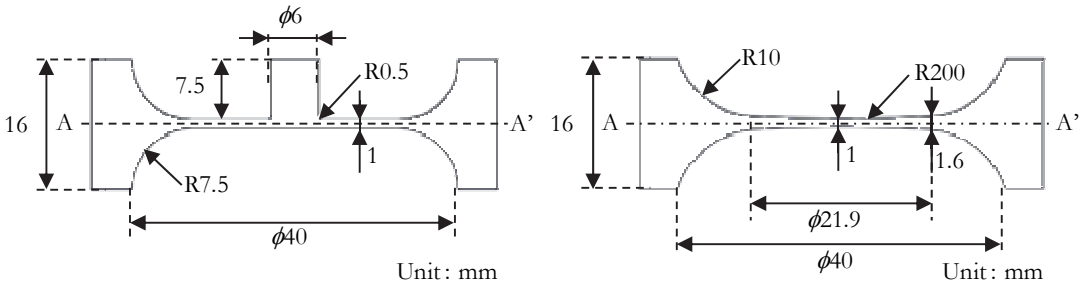

(b) A-A' cross section view of projection type. (c) A-A' cross section view of flat type.

Figure 3: Test specimen.

C	Si	Mn	P	S	Fe
0.16	0.15	0.67	0.012	0.005	Bal.

Table 2: Chemical composition of SS400 in wt. %.

Tensile strength (MPa)	Yield stress (MPa)	Elongation (%)
434	277	32

Table 3: Mechanical properties of SS400.

Method for Reproducing Complex Stress

When reproducing complex stresses or strains with the advanced testing machine, a stress or strain matrix is composed of stress or strain states that are generated by applying a unit load to each axis. In the elastic region, a stress in i direction (σ_i) is described in the following expression using a force in j direction (L_j) and a stress in i direction generated by applying a unit load in j direction ($S_{i,j}$):

$$\begin{bmatrix} \sigma_0 \\ \sigma_{90} \\ \sigma_{45} \end{bmatrix} = \begin{bmatrix} S_{0,0} & S_{0,90} & S_{0,45} \\ S_{90,0} & S_{90,90} & S_{90,45} \\ S_{45,0} & S_{45,90} & S_{45,45} \end{bmatrix} \begin{bmatrix} L_0 \\ L_{90} \\ L_{45} \end{bmatrix} \tag{3}$$

Accordingly, loading conditions ($[L_j]$) for generating arbitrary in-plane stress states ($[\sigma_i]$) generated at the evaluation point of the test specimen are stated as:

$$\begin{bmatrix} L_0 \\ L_{90} \\ L_{45} \end{bmatrix} = \begin{bmatrix} S_{0,0} & S_{0,90} & S_{0,45} \\ S_{90,0} & S_{90,90} & S_{90,45} \\ S_{45,0} & S_{45,90} & S_{45,45} \end{bmatrix}^{-1} \begin{bmatrix} \sigma_0 \\ \sigma_{90} \\ \sigma_{45} \end{bmatrix} \tag{4}$$

The inverse matrix in Eq. (4) is calculated by either measurement results using a rosette gauge by applying a unit load to each axis or numerical results using a FE model with the constraint conditions of the testing machine as shown in Fig. 4.

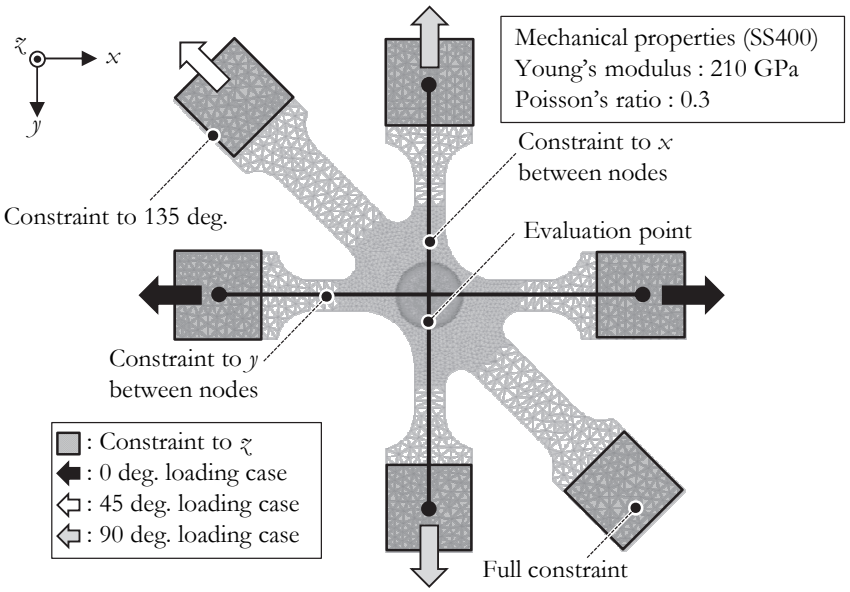

Figure 4: FE model with constraint conditions of testing machine.

EXPERIMENTAL RESULTS AND DISCUSSION

Reproducibility of Complex Stress

Complex stress states were reproduced in the center of the flat type test specimen as shown in Fig 3 (c) by the advanced testing machine. The stress states to be reproduced had been measured using a rosette gauge on the mechanical surface of actual transport machinery in operation. The reproduced stress was compared with the measured stress in Fig. 5. It was found that the reproduced stress history was in good agreement with the measured stress. The errors in each peak stress were within 10 %.

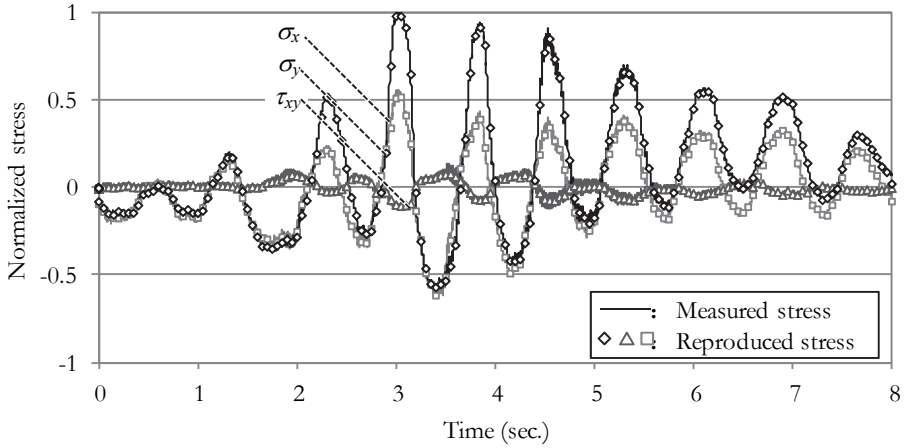

Figure 5: Comparison between reproduced and measured stresses.

Fatigue testing results under non-proportional loading conditions

We made a comparison between measured fatigue lives and predicted fatigue lives under random non-proportional loading conditions.

The fatigue tests were conducted by applying one random waveform for 240 seconds repeatedly. To execute the non-proportional test, the waveform having different amplitude and phase was generated in each axis.

For predicting fatigue lives, two types of stresses, σ_{cr} (Eq. (5)) calculated by critical plane method [5] and σ_{ma} (Eq. (6)) in consideration of the non-proportional level calculated by amplitude and direction of principal stress, were used.

$$\sigma_{cr(t)} = \frac{1}{2}\left(\sigma_{x(t)} + \sigma_{y(t)}\right) + \frac{1}{2}\left(\sigma_{x(t)} - \sigma_{y(t)}\right)\cos(2\varphi_{cr}) + \tau_{xy}\sin(2\varphi_{cr}) \tag{5}$$

$$\sigma_{ma(t)} = \left(1 + \beta \cdot f_{ma}\right)\sigma_{cr(t)} \tag{6}$$

where ϕ_{cr} is the angle between the direction perpendicular to the critical plane and x axis, and β is the material constant expressing the influence of non-proportional loading. f_{ma} is the parameter expressing the intensity of non-proportional loading and described as:

$$f_{ma} = \sqrt{\frac{\int_0^T \left(\sigma_{I(t)} \cdot \sin\left(2\varphi_{I(t)}\right)\right)^2 dt}{\int_0^T \left(\sigma_{I(t)}\right)^2 dt}} \tag{7}$$

where $\sigma_{I(t)}$ is the maximum absolute value of principal stress at time t, and $\phi_{I(t)}$ is the direction of $\sigma_{I(t)}$. Each stress is calculated by numerical results using the FE model shown in Fig. 4. Predicted fatigue lives were calculated using stress cycle counting, i.e. Rainflow method, and linear cumulative damage rule based on the modified Miner's rule.

It was found that predicted fatigue lives with σ_{cr} were over a factor of 10 against measured fatigue lives as shown in Fig. 6. On the other hand, predicted fatigue lives with σ_{ma} were within a factor of 3 against measured fatigue lives. It can be noticed that the errors of predicted fatigue lives using σ_{ma} are caused by the relationship between maximum principal stress and minimum principal stress. The minimum principal stress in condition A (the most conservative as shown in Fig. 6) has the opposite sign as the maximum principal stress. On the other hand, the minimum principal stress in condition B (the most non-conservative as shown in Fig. 6) has the same sign. When the maximum principal stress is tensile, the compressive minimum principal stress has a promoting effect on fatigue crack initiation and propagation. On the other hand, the tensile minimum principal stress has a suppressing effect. The stress states in condition B can only be reproduced in the advanced testing machine; therefore, the advanced testing machine is effective in developing the method for high-accuracy prediction of fatigue life in consideration of the minimum principal stress effect.

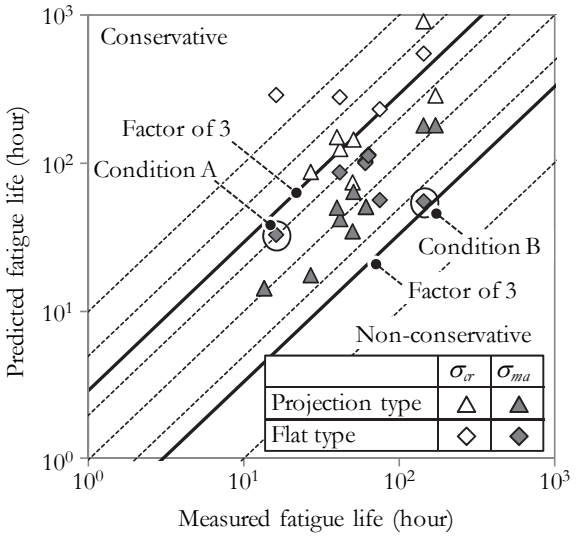

Figure 6: Comparison between predicted fatigue lives and measured fatigue lives.

CONCLUSIONS

1. We have developed a planar tri-axial fatigue testing machine which can reproduce arbitrary in-plane stress states by applying three independent loads in the 0, 45, and 90 degree directions. The complex stress data obtained from actual transport machinery in operation has been reproduced with an error range of less than 10%.
2. Predicted fatigue lives using stress calculated by critical plane method were over a factor of 10 against measured fatigue lives under random non-proportional loading conditions.
3. Predicted fatigue lives using stress in consideration of the non-proportional level were within a factor of 3 against measured fatigue lives.

REFERENCES

[1] Shamsaei, N., Fatemi, A., Socie, D. F., Multiaxial fatigue evaluation using discriminating strain paths, Int. J. Fatigue, 33 (2011) 597–609.
[2] Ahmadzadeh, G.R., Varvani-Farahani, A., Fatigue life assessment of steel samples under various irregular multiaxial loading spectra by means of two energy-based critical plane damage models, Int. J. Fatigue, 84 (2016) 113-121.
[3] Liu, X.-Y., Su, T.-X., Zhang, Y., Yuan, M.-N., A multiaxial high-cycle fatigue life evaluation model for notched structural components, 80 (2015) 443-448.
[4] Gotoh, K., Niwa, T., Anai, Y., Fatigue crack growth behavior of an out-of-plane gusset welded joints under biaxial tensile loadings with different phases, Procedia Materials Science, 3 (2014) 1536-1541.
[5] Susmel, L., Multiaxial Notch Fatigue: from Nominal to Local Stress/Strain Quantities, Woodhead Publishing Limited, Abington Hall, Granta Park, Creat Abington, Cambridge CB21 6AH, UK, (2009).